PROCEEDINGS OF SCIENCE

Beta decay and the r-process

J. Cass, G. Passucci

Department of Physics, University of Notre Dame, Notre Dame, IN 46556

R. Surman
Department of Physics and Astronomy, Union College, Schenectady, NY 12308
Department of Physics, University of Notre Dame, Notre Dame, IN 46556
E-mail: surmanr@union.edu

A. Aprahamian*
Department of Physics, University of Notre Dame, Notre Dame, IN 46556
E-mail: aapraham@nd.edu

Beta decay rates have long been known to be crucial pieces of nuclear data for calculations of *r*-process nucleosynthesis. In light of experimental advances that have pushed measurement capabilities closer to the classic *r*-process path, we revisit the role of individual beta decay rates in a range of potential main *r*-process scenarios. We consider hot *r*-processes characterized by (n,γ)-(γ,n) equilibrium and steady beta flow, and cold r-processes where (n,γ)-(γ,n) equilibrium is estabilshed briefly if at all. We point out the nuclei in each of these scenarios whose beta decay rates have the greatest impact on the overall *r*-process abundance pattern and describe the mechanisms by which this influence occurs.

XII International Symposium on Nuclei in the Cosmos,
August 5-12, 2012
Cairns, Australia

*Speaker.

PoS(NIC XII)154

1. Introduction

It has long been known that the most crucial pieces of nuclear data for simulations of rapid neutron capture, or *r*-process, nucleosynthesis [1, 2] are nuclear masses and beta decay rates. For an *r*-process that proceeds in (n,γ)-(γ,n) equilibrium, nuclear masses determine the nucleus of maximum abundance along each isotopic chain—the *r*-process path. The isotopic chains are connected via beta decays, and so the beta decay rates determine the relative abundances of the nuclei along the *r*-process path. In addition, in this classic picture, the sequence of beta decays along the path set the time required to produce the heaviest elements.

How the *r*-process abundance pattern is shaped by different sets of theoretical calculations of beta decay rates far from stability have been examined by many groups; see [3] for a review and [4] for a recent study. In addition, the impact of newly measured beta decay rates near the *r*-process path has been examined in [5]. Our goal here is complementary to these efforts: to determine the *individual* beta decay rates that have the greatest leverage on the final *r*-process abundance pattern.

2. Sensitivity Study

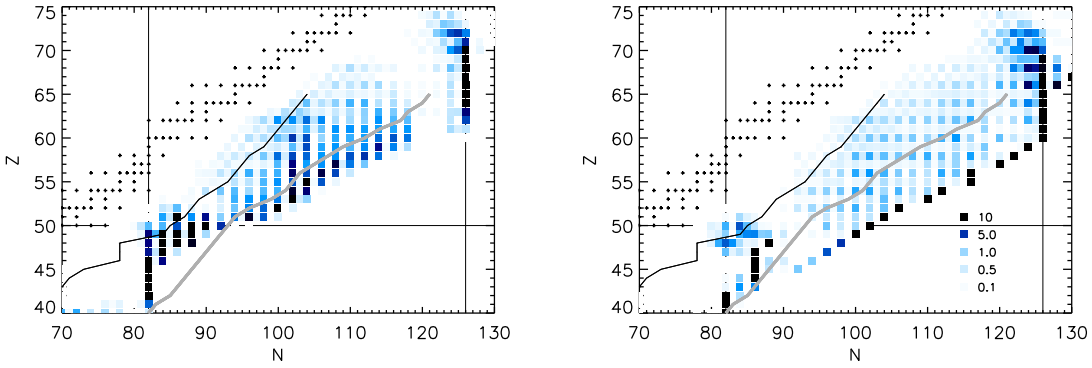

Figure 1: Shows the average sensitivity measure F (Eq. 2.1) for increases and decreases in the beta decay rate by a factor of 10 for each nucleus in the *r*-process network. The darkest squares show $F > 10$. The left panel starts with a hot *r*-process baseline simulation parameterized as in [11] with entropy $s/k = 100$, timescale $\tau = 0.1$ s, and initial $Y_e = 0.26$. The cold example (right panel) is parameterized as in [12] with $s/k = 10$, $\tau = 0.02$ s, and initial $Y_e = 0.2$. Overlaid are the CARIBU[13, 14] (thin black line) and predicted FRIB[15] (thick grey line) accessibility limits (defined as a fission yield greater than 10^{-4}).

To study the influence of individual beta decay rates on the *r*-process abundance distribution, we undertake a sensitivity study similar to that in [6, 7]. For our *r*-process calculations, we use the set of codes described in [6], with masses from [8], capture rates from [9], and beta decay rates from [10]. We chose a baseline simulation that produces a solar-type *r*-process abundance distribution for $A > 120$, then we rerun the simulation with one individual beta-decay rate increased or decreased by a factor of 10. The latter is repeated for each nucleus in the network. We then compare the final abundance patterns to the baseline using the sensitivity measure F:

$$F = 100 \sum_{A} |X_{A,baseline} - X_A| \tag{2.1}$$

where $X_{A,baseline}$ and X_A are the final mass fractions for the baseline simulation and the simulation with the beta decay rate change, respectively.

Fig. 1 shows the results of two such beta decay sensitivity studies. The baseline simulations chosen are representative of two types of *r*-processes: a hot *r*-process that proceeds primarily in (n,γ)-(γ,n) equilibrium, and a cold *r*-process where the temperature and density drop quickly. For the latter case, (n,γ)-(γ,n) equilibrium is established only briefly, though once the photodissociation rates drop out a new equilibrium is established between captures and beta decays [16]. In both examples, the nuclei whose beta decay rates have the largest impact ($F > 10$) tend to lie along the 'equilibrium' *r*-process path, as expected. Additionally, however, we find that sensitivity to beta decay rates stretches to nuclei quite close to stability. This is a result of the competition between beta decay and neutron capture that governs how the *r*-process pattern is finalized during freezeout from equilibrium.

3. Analysis

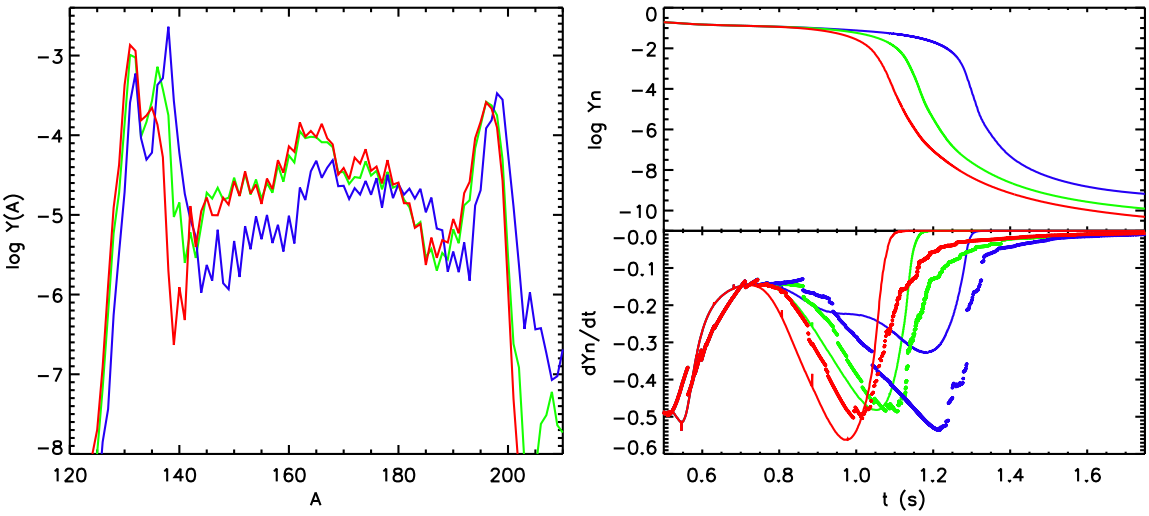

Figure 2: Results from the hot *r*-process baseline simulation (green lines) compared to the simulation repeated with the beta decay rate of ^{140}Sn increased (red) and decreased (blue) by a factor of 10. The left panel shows the final abundance pattern and the top right panel shows the neutron abundance as a function of time. The bottom right panel shows the rate at which neutrons are consumed in the simulation (lines) as compared to the estimated neutron consumption rate from Eq. 3.2 (points).

As shown in Fig. 1, by far the most important beta decay rates are those of nuclei that lie along the *r*-process path. This can be understood from the classic picture of the *r*-process, in which the relative abundances of the nuclei along the *r*-process path are given by the steady beta flow condition:

$$Y(Z,A_{path})\lambda_\beta(Z,A_{path}) \sim \text{constant} \tag{3.1}$$

where $Y(Z,A_{path})$ is the abundance of the isotope of element Z along the *r*-process path and λ_β is its beta decay rate. In addition, the beta decay rates of nuclei along the path roughly determine the

rate at which neutrons are consumed:

$$\frac{dY_n}{dt} \sim -\sum_Z Y(Z,A_{path})\lambda_\beta(Z,A_{path})N' \tag{3.2}$$

where N' is the number of neutrons required to return to the path at $Z+1$ following decay. These approximations hold reasonably well for both of the *r*-process scenarios of Fig. 1, even in the cold *r*-process that falls quickly out of (n,γ)-(γ,n) equilibrium. As a result, the beta decay rates of nuclei along the *r*-process path have the greatest leverage on the final *r*-process pattern as they set the local abundances as well as the overall rate at which neutrons are consumed. Fig. 2 shows an example of this influence of a single beta decay rate.

Individual beta decay rates continue to shape the final *r*-process abundance distribution as the material moves back toward stability, for as long as the timescale for neutron captures remains comparable to the timescale for beta decay. As a result and as shown in Fig. 1, the sensitivity measure F (Eq. 2.1) can be large even for nuclei quite close to stability, particularly near the closed shells and in the rare earth region. These sensitivity measures are very roughly proportional to the time-integrated abundance of the nuclei in the baseline simulation, as shown in the rightmost panel of Fig. 3. This is in contrast to the sensitivities of the *r*-process to other types of nuclear data such as neutron capture rates and neutron separation energies, which show little to no correlation with baseline abundances (left and center panels of Fig. 3).

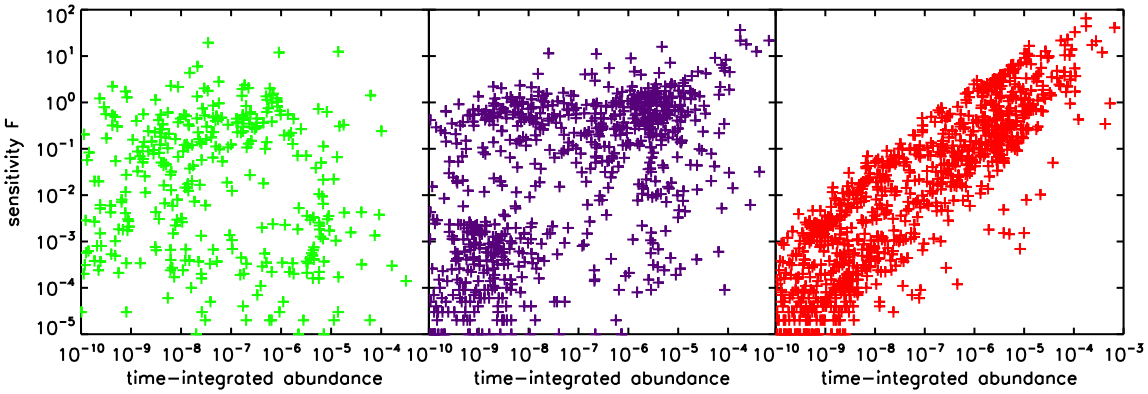

Figure 3: Sensitivity measures F (Eq. 2.1) of the final *r*-process abundance pattern to neutron capture rates (left panel), neutron separation energies (center panel), and beta decay rates (right panel) as a function of the baseline time-integrated abundance of the nucleus whose nuclear physics data is modified. The baseline simulation is the hot *r*-process example in Fig. 1. The capture rates are individually modified by a factor of 100 in the neutron capture rate sensitivity study, as in [6], and the separation energies are modified by 25% in the separation energy study, as in [17].

4. Ongoing work

Current and next-generation radioactive beam facilities will have the capability to measure beta decay rates of neutron-rich nuclei approaching the classic hot *r*-process path (see, e.g., [18, 19, 20, 21], and Fig. 1). Our goal to point out which beta decay rates are most important to measure in these facilities is complicated by the fact that the important beta decay rates for a given

r-process simulation depend on the nuclei that are most abundant in that particular simulation. Since the astrophysical site of the *r*-process is unknown, we are currently examining a wide range of potential *r*-process scenarios. We will perform our sensitivity anaysis for each, and then look for the nuclei whose beta decay rates affect an $F > 1$ change in the widest range of the tested scenarios.

Acknowledgements

This work is supported by the National Science Foundation through grant number PHY0758100 and the Joint Institute for Nuclear Astrophysics grant number PHY0822648.

References

[1] E.M. Burbidge, G.R. Burbidge, W.A. Fowler, and F. Hoyle, *Rev. Mod. Phys.* **29**, 547 (1957).

[2] A.G.W. Cameron, *Chalk River Rep.* **CRL-41** (1957).

[3] M. Arnould, S. Goriely, and K. Takahashi, *Phys. Rep.* **450**, 97 (2007) [arXiv:0705.4512 [astro-ph]].

[4] A. Arcones and G. Martinez-Pinedo, *Phys. Rev. C* **83**, 045809 (2011) [arXiv:1008.3890 [astro-ph.SR]].

[5] N. Nishimura et al., *Phys. Rev. C* **85**, 048801 (2012) [arXiv:1203.5281 [astro-ph.SR]].

[6] R. Surman, J. Beun, G.C. McLaughlin, and W.R. Hix, *Phys. Rev. C* **79**, 045809 (2009) [arXiv:0806.3753 [nucl-th]].

[7] M. Mumpower, G.C. McLaughlin, and R. Surman, *Phys. Rev. C*, accepted (2012) [arXiv:1204.0437 [nucl-th]].

[8] P. Moller, J.R. Nix, W.D. Myers, and W.J. Swiatecki, *Atomic Data Nucl Data Tables* **59**, 185 (1995) [arXiv:nucl-th/9308022].

[9] T. Rauscher and F.-K. Thielemann, *Atomic Data Nucl Data Tables* **74**, 1 (2000) [arXiv:astro-ph/0004059].

[10] P. Moller, B. Pfeiffer, and K.-L. Kratz, *Phys. Rev. C* **67**, 055802 (2003).

[11] B.S. Meyer, *Phys. Rev. C* **89**, 231101 (2002).

[12] I.V. Panov and H.-Th. Janka, *Astron. Astrophys.* **494**, 829 (2009) [arXiv:0805.1848 [astro-ph]].

[13] G. Savard and R. Pardo, *Proposal for the ^{252}Cf source upgrade to the ATLAS facility* (2005).

[14] T.R. England and B.F. Rider, *LA-UR-94-3106*, http://ie.lbl.gov/fission/252Cf.txt

[15] O. Tarasov and M. Hausmann, http://groups.nscl.msu.edu/frib/rates/fribrates.html (2012).

[16] S. Wanajo, *Astrophys. J* **666**, L77 (2007) [arXiv:0706.4360 [astro-ph]].

[17] S. Brett, I. Bentley, N. Paul, A. Aprahamian, and R. Surman, accepted in European Physical Journal A (2012).

[18] P.T. Hosmer et al., *Phys. Rev. Let.* **94**, 112501 (2005) [arXiv:nucl-ex/0504005].

[19] S. Nishimura et al., *Phys. Rev. Let.* **106**, 052502 (2011).

[20] M. Madurga et al., *Phys. Rev. Let.* **109**, 112501 (2012).

[21] M. Thoennessen, *Nucl. Phys. A* **834**, 688 (2010).